Short Communication

# Sol–gel synthesis and characterization of silica supported nickel ferrite catalysts for dry reforming of methane

Rafik Benrabaa [a,b], Axel Löfberg [c,*], Jesús Guerrero Caballero [c], Elisabeth Bordes-Richard [c], Annick Rubbens [c], Rose-Noëlle Vannier [c], Hamza Boukhlouf [a,d], Akila Barama [a]

[a] Laboratoire de Matériaux Catalytiques et Catalyse en Chimie Organique, Faculté de Chimie, USTHB, BP32, El-Alia, Bab Ezzouar, 16111 Alger, Algérie
[b] Université 20 Août-Skikda, Faculté de Technologie, Département de Pétrochimie &Génie des Procédés, BP 26, Route El-Hadaiek, 21000 Skikda, Algérie
[c] Unité de Catalyse et de Chimie du Solide, UMR CNRS 8181, Université Lille 1, Sciences et Technologies, Bât. C3 Cité Scientifique, 59655 Villeneuve d'Ascq, France
[d] Sonatrach, Institut Algérien du Pétrole, Les Platanes Filfila, 21101 Skikda, Algérie

## ARTICLE INFO

## ABSTRACT

Silica-supported $NiFe_2O_4$ spinel was prepared by sol–gel method using tetramethyl orthosilicate as a precursor of silica. B.E.T., XRD, MEB–EDS, TEM, XPS and Raman scattering techniques were used for its characterization. The reducibility by hydrogen was investigated by TPR and HT-XRD. These properties are compared to those of unsupported $NiFe_2O_4$. Both acidic and redox sites were found by studying the decomposition of isopropanol. First experiments in the dry reforming of methane by $CO_2$ showed that owing to more acidic properties supporting $NiFe_2O_4$ on silica provides a more active and selective catalyst that seems less prone to coking.

## 1. Introduction

Though steam reforming of methane to syngas is industrially practiced over the world, dry reforming of methane (DRM) attracts much attention from both environmental and industrial concerns. Nickel is the main active component of most catalysts, but upon sintering particles become large and easily deactivated by coking. A means to reduce the size of Ni particles is to control the reduction of a nickel-containing oxidic matrix [1]. Spinels, perovskites, pyrochlores are typical structural families examined for this purpose [2–6]. Recently we studied several methods of syntheses of $NiFe_2O_4$, some of them allowing the formation of nanoparticles [7–9]. The acid-base properties of $NiFe_2O_4$ determined by decomposition of isopropanol were examined [10–12]. Propene was formed on acidic sites while basic and redox sites led to acetone formation [13,14].

Nanosized particles of ferrites are gaining considerable interest for their properties, beginning by magnetism [15–19]. However, it is difficult to produce uniform and reproducible nanoparticles using traditional methods. In addition, nanoparticles have a strong tendency to agglomerate. A way to solve this problem is to disperse nanoparticles in an oxidic matrix by using sol–gel technique. The latter allows low synthesis temperature, homogenous dispersion and a good control of

stoichiometry. Tetramethyl orthosilicate (TMOS) as a precursor of silica is an excellent host for supporting different kinds of guest nanoparticles [20]. TMOS facilitates the hydrolysis and condensation in the presence of dilute HCl agent, giving homogeneous monolithic and transparent gels [21]. In addition, the porous nature of silica minimizes the phenomenon of aggregation of hosted nanoparticles. We have prepared sol–gel derived nickel ferrite/$SiO_2$ to examine the effect of dispersion on the catalytic properties in DRM reaction. The textural and structural properties, the acid-base character and the catalytic properties are compared to those of unsupported ferrite particles.

## 2. Experimental

### 2.1. Catalysts preparation

Silica supported $NiFe_2O_4$ was synthesized by sol–gel method, using TMOS as the precursor of silica. $Ni(NO_3)_2 \cdot 6H_2O$ (2.9 g) and $Fe(NO_3)_3 \cdot 9H_2O$ (8.1 g) were dissolved in 40 mL ethyl alcohol; this solution was added to 60 mL of TMOS in water (Ni:Fe:$SiO_2$ = 1:2:9). Ten mL of HCl (0.1 M) was added up to pH ~ 2. The wet sols were allowed to gel at room temperature for three weeks. The $10$-$NiFe_2O_4$/$90$-$SiO_2$ gel was dried at 200 °C and calcined at 750 °C for 2 h (NF/$SiO_2$). For comparative purposes, unsupported $NiFe_2O_4$ samples were prepared by hydrothermal (NF–HT) and by sol–gel (NF–SG) syntheses, using the same protocols as previously reported [7–9].

* Corresponding author. Tel.: +33 3 20 43 45 27; fax: +33 3 20 43 65 61.
E-mail address: Axel.Lofberg@univ-lille1.fr (A. Löfberg).

**Table 1**
Textural data of NF/SiO$_2$, NF–HT and NF-SG.

| Catalyst | SSA (m²/g) | A$_p$ (m²/g)[a] | V$_p$ (cm³/g)[b] | r$_p$ (Å)[c] |
|---|---|---|---|---|
| NF/SiO$_2$ | 152 | 108 | 0.049 | 10 |
| NF–HT | 184 | 6.4 | 0.001 | 26 |
| NF–SG | 52 | – | – | 77 |

[a] Micropore area.
[b] Micropore volume.
[c] Average pore radius.

### 2.2. Characterization

The specific surface area and porosity were determined by nitrogen adsorption at −196 °C using BET and BJH methods. SEM–EDS, TEM, XPS, XRD and Raman scattering techniques were used for textural and structural characterization of catalysts. The reducibility of catalysts was examined by TPR-H$_2$ and by H$_2$-HTXRD. Details of the operating conditions may be found in [7–9].

### 2.3. Catalytic experiments

The catalytic conversion of isopropanol was studied between 200 and 400 °C in the absence of oxygen, at atmospheric pressure (ca. 0.05 g of catalyst) [7]. The DRM reaction was investigated using 100 mg of catalyst mixed with SiC loaded in a conventional fixed bed flow reactor. Samples were pre-reduced under 5% H$_2$/He at 400 °C. Effluents were analyzed by mass spectrometry. The diluted reactants (CH$_4$:CO$_2$:He:Ar = 20:10:10:50) were flowed at 90 mL/min rate and GHSV 54 Lh$^{-1}$g$_{cat}^{-1}$ (contact time 0.6 s) at 800 °C.

## 3. Results and discussion

### 3.1. Textural properties

The specific surface area (S$_{BET}$) of NF/SiO$_2$ after calcination at 750 °C and other porosity data are gathered in Table 1. They are compared to unsupported NF samples prepared by hydrothermal synthesis (NF–HT) which delivered directly the spinel [7,8] and by sol–gel method after calcination at 400 °C (NF–SG) [9]. As expected, the value is larger for NF–HT, and S$_{BET}$ decreases along the NF–HT > NF/SiO$_2$ > NF–SG series. The value of porous volume calculated by BJH method is in harmony with SEM picture (Fig. 1-a) which shows aggregates of particles of 0.2 to 5 μm, some of them having a crystalline aspect. In contrast, particles of NF–HT and NF–SG are nanosized (Fig. 1-b, c). Thus the porosity exhibited by NF/SiO$_2$ seems to be mostly due to silica.

### 3.2. Structural properties

The diffractograms of NF/SiO$_2$, NF–HT and NF–SG are presented in Fig. 2. Though the pattern of NF/SiO$_2$ is blurred, all lines could be assigned to NiFe$_2$O$_4$ (PDF 00-054-0964); silica which is amorphous was recognized by a hump at ca. 2θ = 22.5° [22]. These figures suggest that particles of NiFe$_2$O$_4$ have nucleated in the silica matrix. No line corresponding to nickel or iron oxides, quartz, cristobalite or mixed compounds like SiFe$_2$O$_4$ could be observed.

The Raman spectra of NF/SiO$_2$ calcined at 750 °C and of NF samples (Fig. 3) show the bands located at 335, 459, 488, 570, 589, 664 and 701 cm$^{-1}$ characteristic of NiFe$_2$O$_4$. The strong band at 701 cm$^{-1}$, assigned to the symmetrical stretching motion of [FeO$_4$] tetrahedral unit, is the fingerprinting of NiFe$_2$O$_4$ inverse spinel [23,24]. These results are in good agreement with XRD analysis.

### 3.3. Surface properties

The surface composition was determined by XPS (Table 2). The presence of Ni$^{2+}$, Fe$^{3+}$ and Si$^{4+}$ was detected by Ni 2p$^{3/2}$ (854.9–855.8 eV), Fe 2p$^{3/2}$ (710.1–710.7 eV) and Si 2p$^{3/2}$ (103,7–103,9 eV) photopeaks, respectively [25,26]. Surface atomic ratios were calculated. In NF/SiO$_2$, Fe/Ni is smaller than 2, the expected value for NiFe$_2$O$_4$, as compared to bulk NF samples (Table 2). About a third of Fe$^{3+}$ lacks and conversely two thirds of surface species would be nickel (II) species. Si/Fe is higher but Si/Ni is lower than the respective theoretical values. As a conclusion, Ni$^{2+}$ species (may be as nanosized particles of NiO undetectable by XRD) and NiFe$_2$O$_4$ particles are mostly embedded, and not properly supported on silica.

### 3.4. Reducibility in hydrogen

The reducibility of NF/SiO$_2$ examined by H$_2$-TPR is clearly different from that of NF–HT and NF–SG catalysts (Fig. 4). The amount of consumed H$_2$ is 16–17 μmol/g for both NF–HT and NF–SG whereas it is smaller for NF/SiO$_2$ (2.6 μmol/g). The TPR profiles also are different. Well-defined steps of reduction are observed during the reduction of bulk NiFe$_2$O$_4$ (NF–HT and NF–SG), reactions being assigned to them in Fig. 4. For NF/SiO$_2$, these peaks are replaced by a broad one located in the 300–800 °C range which is attributed to the reduction of Ni$^{2+}$ and Fe$^{3+}$ species and/or of NiFe$_2$O$_4$ nanoparticles dispersed inside silica matrix. Though XPS indicated that Ni$^{2+}$ species are more numerous on surface (Fe/Ni = 0.6) than for NF–SG and NF–HT (Fe/Ni = 2.3 and 1.8, respectively) it is difficult to put in evidence their own reduction.

In situ H$_2$-HTXRD of NF/SiO$_2$ was performed up to 800 °C. The temperatures of reduction of Ni$^{2+}$ and of the formation of γ − Ni–Fe alloy are not that different from those of unsupported nickel ferrite [8,9]. The diffractograms (Fig. 5) show that silica supported NiFe$_2$O$_4$ is stable up to 400 °C. At 450 °C, the line at 2θ ~ 44° of metallic Ni species starts to grow, as well as the formation of γ − Ni–Fe, identified by the peaks at 2θ ~ 43 and ~50°. Metallic nickel disappears at ca. 600 °C.

### 3.5. Catalytic decomposition of isopropanol

Table 3 shows the conversion of isopropanol, the distribution of products and the rates of formation of propylene and acetone of NF/SiO$_2$ and NF–HT. Propylene and acetone are the main products. Isopropanol decomposition begins at 200 °C, its conversion being higher for NF/SiO$_2$ than for NF–HT. The rate of formation of propylene
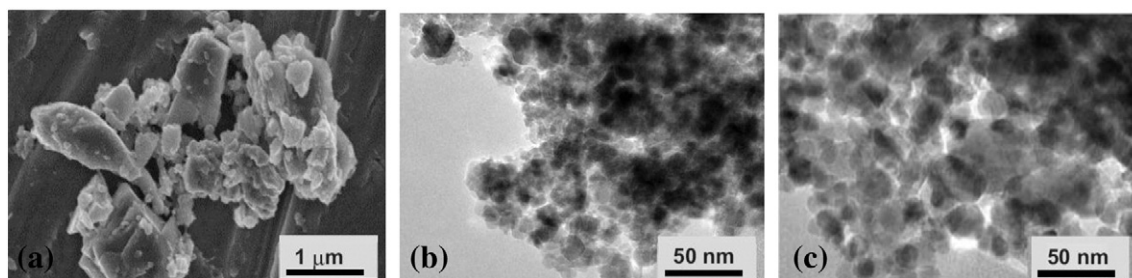


**Fig. 1.** SEM picture of NF/SiO$_2$ (a); TEM pictures of NF–HT (b) and NF–SG (c).